Accelerated Publication

THE JOURNAL OF BIOLOGICAL CHEMISTRY
Vol. 278, No. 19, Issue of May 9, pp. 16462–16465, 2003

Direct Observation of Amyloid Fibril Growth Monitored by Thioflavin T Fluorescence*[S]

Received for publication, February 3, 2003,
and in revised form, March 18, 2003
Published, JBC Papers in Press, March 18, 2003,
DOI 10.1074/jbc.C300049200

Tadato Ban‡§, Daizo Hamada‡§¶, Kazuhiro Hasegawa‖, Hironobu Naiki‖, and Yuji Goto‡**

From the ‡Institute for Protein Research, Osaka University and Core Research for Evolutional Science and Technology (CREST), Japan Science and Technology Cooperation, 3-2 Yamadaoka, Suita, Osaka 565-0871, Japan and the ‖Department of Pathology, Fukui Medical University and CREST, Japan Science and Technology Corporation, Matsuoka, Fukui 910-1193, Japan

Real-time monitoring of fibril growth is essential to clarify the mechanism of amyloid fibril formation. Thioflavin T (ThT) is a reagent known to become strongly fluorescent upon binding to amyloid fibrils. Here, we show that, by monitoring ThT fluorescence with total internal reflection fluorescence microscopy (TIRFM), amyloid fibrils of β2-microgobulin (β2-m) can be visualized without requiring covalent fluorescence labeling. One of the advantages of TIRFM would be that we selectively monitor fibrils lying along the slide glass, so that we can obtain the exact length of fibrils. This method was used to follow the kinetics of seed-dependent β2-m fibril extension. The extension was unidirectional with various rates, suggesting the heterogeneity of the amyloid structures. Since ThT binding is common to all amyloid fibrils, the present method will have general applicability for the analysis of amyloid fibrils. We confirmed this with the octapeptide corresponding to the C terminus derived from human medin and the Alzheimer's amyloid β-peptide.

There is an increasing body of evidence showing that many proteins including the Alzheimer's amyloid β-peptide (Aβ),[1] prion protein, transthyretin, and β2-microgobulin (β2-m) tend to misfold and aggregate into amyloid fibrils (1–3). Moreover, several proteins not known to be involved in disease and various polyamino acids have been shown to form amyloid fibrils *in vitro* under carefully selected conditions (4, 5). Although no sequence or structural similarity between the amyloid precursor proteins has been found, amyloid fibrils share several common structural and spectroscopic properties (6). Irrespective of the protein species, electron microscopy and x-ray fiber diffraction indicate that the amyloid fibrils have relatively rigid structures with diameters of 10–15 nm consisting of cross-β-strands. Making use of an NMR technique in combination with hydrogen/deuterium exchange of amide protons and dissolution of amyloid fibrils by dimethyl sulfoxide, we have shown that the amyloid fibrils of β2-m are stabilized by a hydrogen-bond network which is more extensive than that in the native state (7).

Amyloid fibril formation is considered to be a nucleation-dependent process in which non-native precursor proteins slowly associate to form the nuclei (8). This process is followed by an extension reaction, where the nucleus grows by sequential incorporation of more precursor protein molecules. This model has been validated by the observation that fibril extension kinetics is accelerated by the addition of preformed fibrils, *i.e.* by a seeding effect. However, the mechanism of fibril formation by individual polypeptide chains is not completely understood, and there are several variations of the nucleation-dependent model (9, 10). To address the mechanism of amyloid fibril formation, it is important to observe the process at the single-fibril level. Recently, epifluorescence with a newly introduced fluorescent dye (11) and atomic force microscopy (AFM) (12, 13) have been utilized for the direct observation of individual amyloid fibrils. Although these techniques are quite useful in providing information on the mode of fibril growth, the need to introduce the fluorescence probe prevents their general application. On the other hand, the strong interaction of amyloid proteins and the mica surface used in AFM measurements resulted in the formation of fibrils morphologically different from the intact amyloid fibrils (13).

ThT is known to bind rapidly to amyloid fibrils accompanied by a dramatic increase of fluorescence at around 485 nm, when excited at 455 nm (14). This makes ThT one of the most useful probes to detect the formation of amyloid fibrils. Fluorescence at around 485 nm becomes useful in fluorescence microscopic studies, which make use of lasers for the incident beam of excitation. On the other hand, TIRFM has been developed to monitor single molecules (15, 16) by effectively reducing the background fluorescence under the evanescent field formed on the surface of slide glass (Fig. 1). By combining amyloid fibril-specific ThT fluorescence and TIRFM, it would be possible to observe the amyloid fibrils and their formation process without introducing any fluorescence reagent covalently bound to the protein molecule. We examined this possibility using the β2-m amyloid fibrils.

* This work was supported by grants-in-aid for scientific research from the Japanese Ministry of Education, Science, Culture and Sports. The costs of publication of this article were defrayed in part by the payment of page charges. This article must therefore be hereby marked "*advertisement*" in accordance with 18 U.S.C. Section 1734 solely to indicate this fact.

[S] The on-line version of this journal (available at http://www.jbc.org) contains a movie file (b2m.mov): the growth processes of amyloid fibrils monitored by ThT fluorescence with total internal reflection fluorescence microscopy, as shown in Fig. 2, *E–H*.

§ These authors contributed equally.

¶ Supported by Japan Society for Promotion of Science Research Fellowships for Young Scientists. Present address: Dept. of Developmental Infectious Diseases, Research Inst. and Osaka Medical Center for Maternal and Child Health, 840 Murodo-cho, Izumi, Osaka 594-1011, Japan.

** To whom correspondence should be addressed: Inst. for Protein Research, Osaka University 3-2 Yamadaoka, Suita, Osaka 565-0871, Japan. Tel.: 81-6-6879-8614; Fax: 81-6-6879-8616; E-mail: ygoto@protein.osaka-u.ac.jp.

[1] The abbreviations used are: Aβ, amyloid β-peptide; β2-m, β2-microgobulin; AFM, atomic force microscopy; TIRFM, total internal reflection fluorescence microscopy; medC, C terminus derived from human medin; EM, electron microscopy.

EXPERIMENTAL PROCEDURES

Proteins—Recombinant human β2-m with four additional residues at the N-terminal (Glu^{-4}-Ala^{-3}-Tyr^{-2}-Vla^{-1}-Ile^{1}) was expressed and purified as described (17, 18). Synthesized medC fragment (NFGSVQFV) and Aβ-(1–40) were purchased from Peptide Institute, Inc. (Osaka, Japan). The purities of the peptides were >95% according to elution patterns of high performance liquid chromatography.

Fluorescence Microscopy—The fluorescence microscopic system used to observe individual amyloid fibrils was developed based on an inverted microscope (IX70; Olympus, Tokyo, Japan) as described previously (16). The ThT molecule was excited using an argon laser (model 185F02-ADM; Spectra Physics, Mountain View, CA). The fluorescent image was filtered with a bandpass filter (D490/30 Omega Optical, Brattleboro, VT) and visualized using an image intensifier (model VS4–1845; Video Scope International, Sterling, VA) coupled with a SIT camera (C2400–08; Hamamatsu Photonics, Shizuoka, Japan).

Direct Observation of Amyloid Fibrils—β2-m amyloid fibrils were prepared as described previously (17, 18). Seed fibrils prepared by the fragmentation of amyloid fibrils were mixed with 25 μM monomeric β2-m in polymerization buffer (50 mM sodium citrate, pH 2.5, and 100 mM KCl) at 37 °C. After 6-h incubation, the sample solution was diluted 10-fold with polymerization buffer, and 100 μM ThT was added at the final concentration of 5 μM. An aliquot (14 μl) of sample solution was deposited on quartz slide glass, and the fibril image was obtained with TIRFM. All images were recorded on digital videotape and analyzed using Image-pro Plus (Media Cybernetics, Silver Spring, MD).

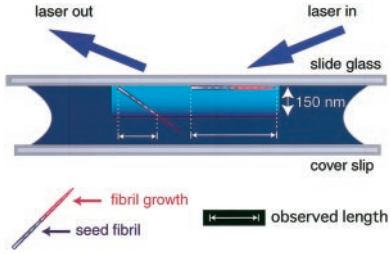

FIG. 1. **Schematic representation of amyloid fibrils by total internal reflection fluorescence microscopy.** The penetration depth of the evanescent field formed by the total internal reflection of laser light is ~150 nm for laser light at 455 nm, so that only amyloid fibrils lying in parallel with the slide glass surface were observed.

Aβ-(1–40) amyloid fibrils were prepared from synthetic Aβ-(1–40) (19). To obtain seed, preformed fibrils were fragmented by sonication as described above. The seeds were added at a final concentration of 10 μg/ml to 50 μM monomeric Aβ-(1–40) in 50 mM sodium phosphate buffer at pH 7.5 and 100 mM NaCl. After 3-h incubation at 37 °C in the test tube, the solution was diluted 5-fold, and ThT was added at a final concentration of 5 μM. The fibril formation of β2-m or Aβ-(1–40) on the slide glass was also examined.

Time-lapse Observation of Amyloid Fibrils —In the case of β2-m, seed fibrils were mixed with 50 μM monomeric β2-m in polymerization buffer (50 mM sodium citrate at pH 2.5 and 100 mM KCl). After ThT was added at 5 μM, the solution was deposited on quartz slide glass, and the growth of individual fibrils was observed every 15 min under a microscope at 37 °C. For medC, seed fibrils were prepared by incubating the monomeric peptide at 1 mM in 10 mM sodium phosphate buffer, pH 7.0, at 37 °C for 24 h. The fibrils were fragmented by a sonicator as described above. An aliquot (1 μl) of the seed solution was mixed with 1 mM medC monomer in the same buffer containing 5 μM ThT and deposited on quartz slide glass at 37 °C for visualization with TIRFM. The images of amyloid fibrils grown under TIRFM recorded on digital video tape were captured on a personal computer and the lengths of the fibrils were calculated using Image-pro Plus.

RESULTS AND DISCUSSION

ThT Observation of β2-m Amyloid Fibrils—β2-m, a 99-residue protein with a typical immunoglobulin domain fold (20), is the light chain of the major histocompatibility complex class I antigen. However, it is also found as a major component of

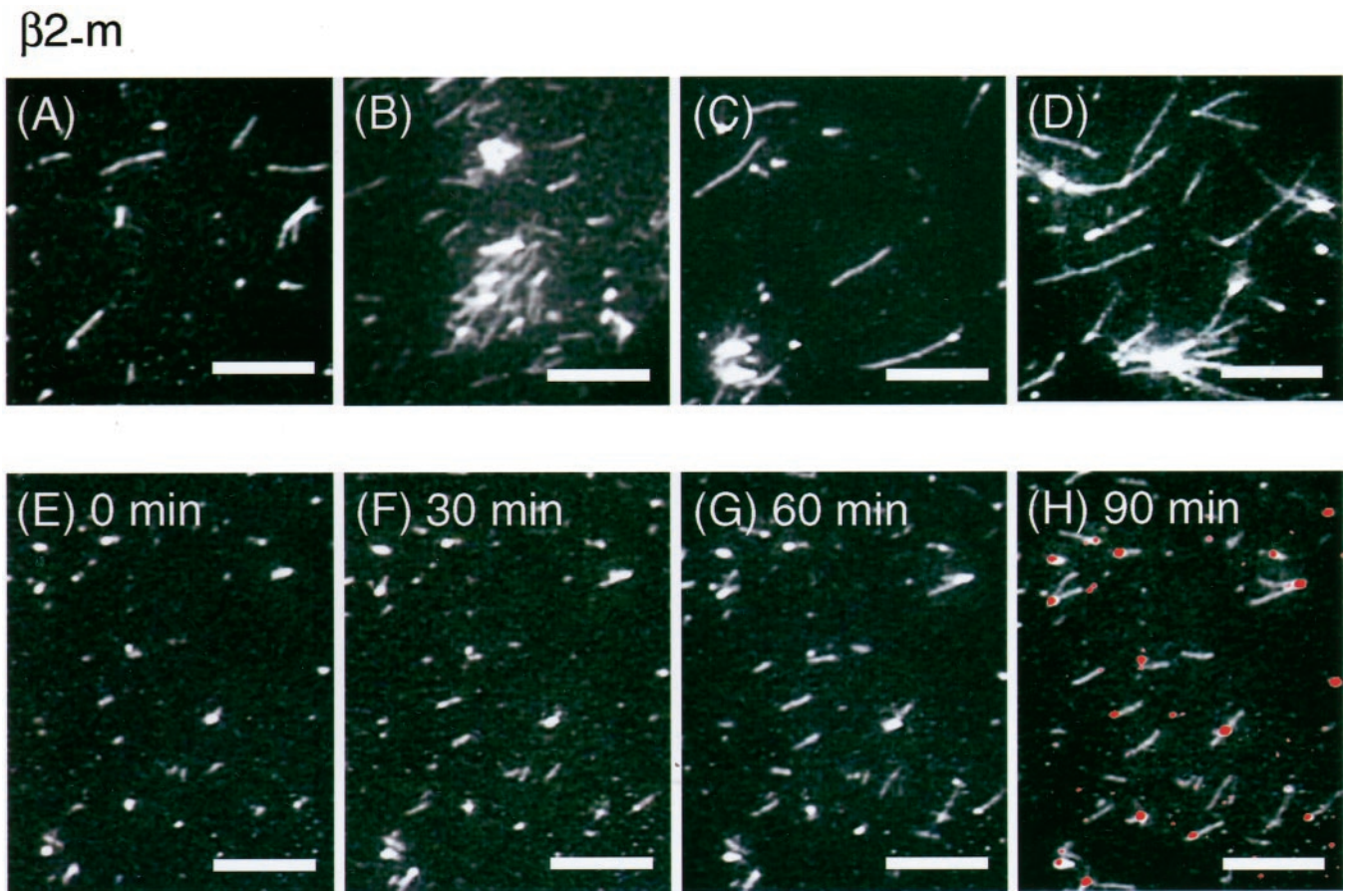

FIG. 2. **Images of β2-m amyloid fibrils observed by ThT fluorescence and TIRFM.** Amyloid fibrils were prepared in a test tube (*A* and *B*) and on glass slides (*C* and *D*). *E–H*, growth processes of amyloid fibrils. Incubation times are 0 (*E*), 30 (*F*), 60 (*G*), and 90 (*H*) min. In *H*, ThT fluorescence at time 0 was overlaid in red to identify the locations of seed fibrils. The *scale bars* are 10 μm.

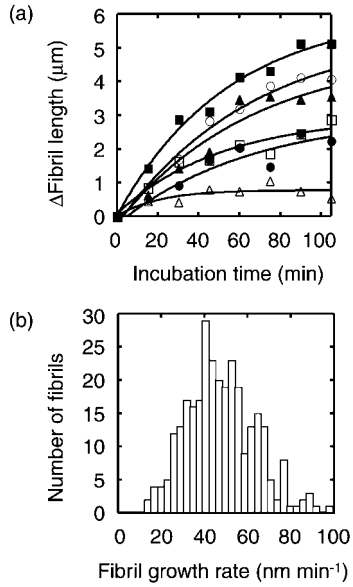

FIG. 3. **Kinetics of β2-m amyloid fibril growth.** *a*, fibril length *versus* incubation time. *Lines* show the fitting to the pseudo first-order kinetics. *b*, histogram for the distribution of the initial fibril growth rate.

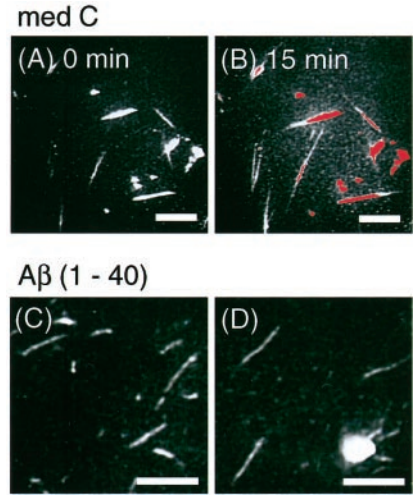

FIG. 4. **Applicability of the ThT method to other amyloid fibrils.** *A* and *B*, seed-dependent fibril growth of medC. Aβ-(1–40) amyloid fibrils were prepared in a test tube (*C*) or on a glass slide (*D*). In *B*, the locations of seed fibrils are indicated by *red*.

amyloid fibrils deposited in dialysis-related amyloidosis, a common and serious complication in patients receiving hemodialysis for more than 10 years (8, 21). Although the exact mechanism of the β2-m amyloid fibril deposition *in vivo* is still unknown, amyloid fibrils are easily formed *in vitro* by a seed-dependent extension reaction at pH 2.5, in which acid-unfolded monomeric β2-m is added to seed fibrils taken from patients (8, 17, 18).

We first examined the β2-m amyloid fibrils already extended in test tubes (Fig. 2, *A* and *B*). TIRFM images indicated the presence of 1–5-μm-long fibrils in the presence of ThT. No such fibrillar structures were found either in the absence of ThT or in the absence of fibrils. This indicated that amyloid-specific fluorescence from ThT enables one to visualize the β2-m amyloid fibrils.

Intriguingly, the length range of the detected fibrils is similar to that observed with electron microscopy (EM) (8, 17) or AFM (18). This indicates that the evanescent field is very useful for determining the length of amyloid fibrils. To obtain the exact length of fibrils by conventional epifluorescence microscopy, one has to analyze the image by three-dimensional reconstruction because the orientation of fibrils relative to slide glass is not always parallel to the glass surface. In contrast, since the penetration depth of the evanescent field formed by the total internal reflection of laser light is quite shallow (~150 nm for laser light at 455 nm) in comparison with the width of amyloid fibrils (~15 nm from EM), TIRFM selectively monitors long fibrils lying along the slide glass (Fig. 1). Consequently, the length of observed fibrils is close to the exact length. On the other hand, the apparent width of the fibrils observed by fluorescence was larger than the exact width because the observed emission fields extend the dye localization.

We then determined whether β2-m amyloid fibrils also formed on the slide glass. Goldsbury *et al.* (13) reported using synthetic human amylin that amylin fibrils that assembled on a mica surface for AFM measurement exhibited distinct morphological features. The seeds, *i.e.* fragmented fibrils, were mixed with monomeric β2-m and immediately the solution was deposited on quartz slide glass. As can be seen, the amyloid fibrils extended on the slide glass with an incubation time of 6 h (Fig. 2, *C* and *D*) were similar to those prepared in the test tube (Fig. 2, *A* and *B*).

Kinetics of Fibril Extension—We monitored the seed-dependent extension reaction (Fig. 2, *E–H*; also see movie b2m.mov, which is published in the Supplemental Material). At time 0, we identified the location of seeds. As we increased the incubation time, we could clearly follow the extension of fibrils: the extension ended at around 2 h under the conditions used. This fact constitutes direct evidence that the fibril formation by β2-m is a seed-dependent process, as suggested for other amyloid fibrils (9–11, 13). A majority of extended β2-m fibrils exhibited unidirectional elongation from the seeds which were marked with red (Fig. 2*H*). Moreover, when the fibrils with bidirectional elongation were observed, the superposition of the seeds was suggested. Therefore, we can conclude that the elongation is mostly unidirectional.

Unidirectional fibril formation was first observed using Sup35, a yeast prion determinant, by epifluorescence microscopy (11). However, another group reported the bidirectional elongation of Sup35 based on the observations with EM in conjunction with selective staining by gold particles (9). Although we cannot exclude the possibility that the interaction with the glass surface was responsible for the unidirectional extension, the unidirectional picture is likely to hold for the fibril formation of β2-m. The unidirectional elongation was also dominant in the formation of fibrils by medC (see below).

The rate of extension of individual amyloid fibrils was analyzed by plotting the length of fibrils as a function of time (Fig. 3*a*). For the respective fibrils, the extension reaction could be well fitted to a single exponential curve, consistent with a previous observation of the seed-dependent extension reaction in test tubes (8, 17, 18). Importantly, the rates of fibril extension, however, varied significantly depending on the fibrils, although the rate for each fibril remained constant. The initial fibril growth rate showed a wide distribution with a mean value of 47.4 ± 15.0 nm min^{-1} (Fig. 3*b*), which cannot be explained by the statistical distribution of the fibril growth rate. Taking into account the fact that the extension rate for each fibril is constant, the diversity in the rate may be related to the difference in the structure of individual fibrils. Recently, the direct observation of fibril formation by AFM indicated that the fibril-forming region of Sup35 forms a diverse population of fibrils that could be distinguished on the basis of their kinetic properties, including polarity and elongation rate (10). Fur-

thermore, another study with NMR (22) indicated that amyloid fibrils formed by the Aβ-(25–35) peptide exhibit a heterogeneity in the kinetics of their hydrogen/deuterium exchange behavior for each amide group. Thus, current data obtained for β2-m as well as the results discussed for Sup35 and Aβ peptide suggest that heterogeneity of structure is a common characteristic of amyloid fibrils. This could be partly consistent with the idea that the rate of crystal growth may be affected by bonding topology at the crystal surface (23).

Medin Fragment and Aβ-(1–40)—To confirm the overall applicability of this method, we examined two other amyloid fibrils. One is medC corresponding to the C-terminal octapeptide of medin (24). Medin, a 50 amino acid internal cleavage peptide of lactadherin, is a component of the very common age-related amyloidosis deposited on the aortic wall. It has been shown that the C-terminal 8-amino acid peptide NFGSVQFV from human medin is associated with amyloid fibrils at neutral pH, 37 °C (24). We first prepared the seed fibrils. In the case of medC, it was difficult to prepare extensively fragmented seeds by sonication. This might be related to the very rigid and sharp morphology of the medC fibrils. The extension reaction was monitored every 5 min under microscopic conditions (Fig. 4, *A* and *B*). We observed the extension of the fibrils, which was mostly unidirectional as was the case for β2-m. Analysis of the extension rate also indicated significant heterogeneity of the extension rate (data not shown).

Another example is Aβ (Fig. 4, *C* and *D*). The intracerebral accumulation of Aβ as senile plaques or vascular amyloid is one of the dominant characteristics in the pathogenesis of Alzheimer's disease (19). Aβ-(1–40) fibrils prepared in test tubes and on slide glass, both by the extension reaction, were compared. Fibrillar structures specifically stained by ThT were formed both in the test tube (Fig. 4*C*) and on the slide glass (Fig. 4*D*). On the slide glass, we often observed clustered aggregates even in the presence of seeds.

In conclusion, we reported a new method to visualize the amyloid fibrils at the single fibril level. The method makes use of the specific ThT binding to amyloid fibrils and TIRFM. Since ThT binding is common to all amyloid fibrils, the present method will have general applicability for the analysis of amyloid fibrils. One of the advantages of TIRFM is that only amyloid fibrils lying in parallel with the slide glass surface were observed, so that we can obtain the exact length of fibrils. Consequently, the method will be particularly important for following the rapid kinetics of fibril formation, which is paramount to elucidating the mechanism of amyloid fibril formation and little accessible by other approaches.

Acknowledgments—We thank T. Wazawa and A. Fernández for valuable discussions.

REFERENCES

1. Sipe, J. D. (1992) *Annu. Rev. Biochem.* **61,** 947–975
2. Hammarstrom, P., Schneider, F., and Kelly, J. W. (2001) *Science* **293,** 2459–2462
3. Dobson, C. M. (2002) *Nature* **418,** 729–730
4. Hamada, D., and Dobson, C. M. (2002) *Protein Sci.* **11,** 2427–2436
5. Fändrich, M., and Dobson, C. M. (2001) *EMBO J.* **21,** 5682–5690
6. Sunde, M., and Blake, C. (1997) *Adv. Protein Chem.* **50,** 123–159
7. Hoshino, M., Katou, H., Hagihara, Y., Hasegawa, K., Naiki, H., and Goto, Y. (2002) *Nat. Struct. Biol.* **9,** 332–336
8. Naiki, H., Hashimoto, N., Suzuki, S., Kimura, H., Nakakuki, K., and Gejyo, F. (1997) *Amyloid* **4,** 223–232
9. Scheibel, T., Kowal, A. S., Bloom, J. D., and Lindquist, S. L. (2001) *Curr. Biol.* **11,** 366–369
10. Depace, A. H., and Weissman, J. S. (2002) *Nat. Struct. Biol.* **9,** 389–396
11. Inoue, Y., Kishimoto, A., Hirao, J., Yoshida, M., and Taguchi, H. (2001) *J. Biol. Chem.* **276,** 35227–35230
12. Ionescu-Zanetti, C., Khurana, R., Gillespie, J. R., Petrick, J. S., Trabachino, L. C., Minert, L. J., Carter, S. A., and Fink, A. L. (1999) *Proc. Natl. Acad. Sci. U. S. A.* **96,** 13175–13179
13. Goldsbury, C., Kistler, J., Aebi, U., Arvinte, T., and Cooper, G. J. (1999) *J. Mol. Biol.* **285,** 33–39
14. Naiki, H., Higuchi, K., Hosokawa, M., and Takeda, T. (1989) *Anal. Biochem.* **177,** 244–249
15. Funatsu, T., Harada, Y., Tokunaga, M., Saito, K., and Yanagida, T. (1995) *Nature* **374,** 555–559
16. Yamasaki, R., Hoshino, M., Wazawa, T., Ishii, Y., Yanagida, T., Kawata, Y. Higurashi, T., Sakai, K., Nagai, J., and Goto, Y. (1999) *J. Mol. Biol.* **292,** 965–972
17. Kozhukh, G. V., Hagihara, Y., Kawakami, T., Hasegawa, K., Naiki, H., and Goto, Y. (2002) *J. Biol. Chem.* **277,** 1310–1315
18. Katou, H., Kanno, T., Hoshino, M., Hagihara, Y., Tanaka, H., Kawai, T., Hasegawa, K., Naiki, H., and Goto, Y. (2002) *Protein Sci.* **11,** 2219–2229
19. Hasegawa, K., Yamaguchi, I., Omata, S., Gejyo, F., and Naiki, H. (1999) *Biochemistry* **38,** 15514–15521
20. Bjokman, P. J., Saper, M. A., Samraoui, B., Bennett, W. S., Strominger, J. L., and Willy, D. C. (1987) *Nature* **329,** 506–512
21. Gejyo, F., Yamada, T., Odani, S., Nakagawa, Y., Arakawa, M., Kunitomo, T., Kataoka, H., Suzuki, M., Nirasawa, Y., Shirahama, T., Cohen, A. S., and Schmid, K. (1985) *Biochem. Biophys. Res. Commun.* **129,** 701–706
22. Ippel, J. H., Olofsson, A., Schleucher, J. S., Lundgren, E., and Wijmenga, S. S. (2002) *Proc. Natl. Acad. Sci. U. S. A.* **99,** 8648–8653
23. Grimbergen, R. F. P., Bennema, P., and Meekes, H. (1999) *Acta Crystallogr. Sect. A* **55**, 84–94
24. Häggqvist, B., Näslund, J., Sletten, K., Westermark, G. T., Mucchiano, G., Tjernberg, L. O., Nordstedt, C., Engström, U., and Westermark, P. (1999) *Proc. Natl. Acad. Sci. U. S. A.* **96,** 8669–8674

Direct Observation of Amyloid Fibril Growth Monitored by Thioflavin T Fluorescence

Tadato Ban, Daizo Hamada, Kazuhiro Hasegawa, Hironobu Naiki and Yuji Goto

J. Biol. Chem. 2003, 278:16462-16465.
doi: 10.1074/jbc.C300049200 originally published online March 18, 2003
